2014 IEEE International Conference on Robotics & Automation (ICRA)
Hong Kong Convention and Exhibition Center
May 31 - June 7, 2014. Hong Kong, China

A Novel Singularity-Consistent Inverse Kinematics Decomposition for S-R-S Type Manipulators

Shota Taki and Dragomir Nenchev

***Abstract*— This paper addresses velocity-level redundancy resolution for S-R-S type redundant manipulators, aiming at precise path following in the presence of kinematic singularities. A novel joint-velocity decomposition scheme that complements and avoids some drawbacks of a previous study based on the Singularity-Consistent method is introduced. As a result, it becomes possible to follow almost any singular path in workspace, including paths passing through bifurcations (nondegenerate singular paths). Further on, the algorithmic singularity introduced in the previous study (the "inner obstacle") disappears in the new formulation. The problem of wrist singularity is also addressed and solved via a proper self motion component. Only a limited subset of singular paths cannot be handled with the method: those that pass through the double elbow-wrist singularity (an isolated point at the workspace boundary). The effectiveness of the proposed method is illustrated via numerical simulations.**

I. Introduction

Many robotic systems comprise S-R-S type structural components. Representative examples are standalone industrial manipulators like PA-10 [1] or the DLR arm [2] and humanoid robots with 7-DOF arms [3], [4]. Inverse kinematics are essential to the control of such manipulators based on workspace coordinates. The singularity problem, however, is an inherent problem in inverse kinematics. Possible approaches to deal with the problem were proposed first for non-redundant manipulators, e.g. the damped least-squares method [5], [6] or similar methods [7], [8]. However, as shown in [9], a directional error occurs in the vicinity of the singularity due to the damping factor. A method to minimize the directional error was proposed in [10]. But nevertheless, the directional error does not precisely become zero. Based on a work by Kieffer [11], the Singularity-Consistent (SC) method [12] was proposed which restricts the magnitude of the end-effector velocity in proportion to the determinant of the Jacobian while following a degenerate singular path. With this method, no directional error arises and the path can be followed precisely, while the end-effector velocity magnitude becomes instantaneously null at the singular point. When following a nondegenarate singular path, however, a vanishing vector field problem arises. An approach to the problem via a switching method based on second-order inverse kinematics has been described in [9].

In the case of redundant manipulators, inverse kinematics in the presence of singularities requires a somewhat different approach as the self motion can be used to alleviate the problem. Many studies are available, e.g. based on screw theory [13], [14], using analytical [15], [16] or numerical solutions [17]. In [18], the SC method was applied to the positioning subchain of a S-R-S type manipulator. Although the proposed solution made it possible to approach and move through the unavoidable "elbow" singularity following degenerate singular paths, an algorithmic singularity (the "inner obstacle") was generated.

The authors are with the Graduate School of Engineering, Tokyo City University, Tamazutsumi 1-28-1, Setagaya-ku, Tokyo 158-8557, Japan.

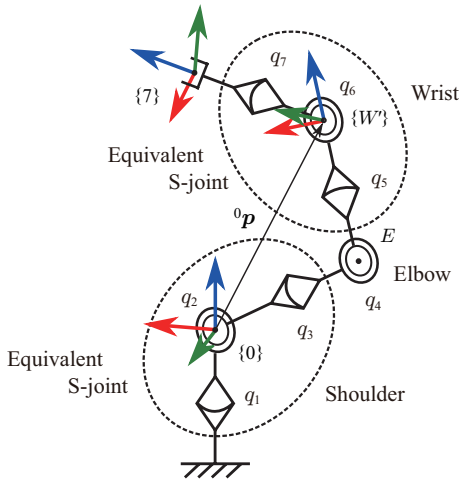

Fig. 1. Kinematic structure of S-R-S type manipulator.

In this paper, we propose a novel type inverse kinematics decomposition that avoids this drawback and that ensures the following of nondegenerate singular paths as well. In addition, the method makes use of the redundancy to avoid the internal wrist singularity. The paper is organized as follows. In Section 2, we establish the mathematical model and highlight the singularity problem of the S-R positioning subchain. In Section 3, we formulate the novel inverse kinematics decomposition for the positioning subchain. Section 4 gives the complete solution, including orientation. Section 5 illustrates the performance via numerical simulations. Finally, we summarize the results in Section 6.

II. Mathematical Model and Kinematic Relation

An S-R-S type anthropomorphic manipulator comprises a relatively simple structure, similar to that of the human arm. As shown in Fig. 1, the manipulator is composed of seven revolute joints. The first three and the last three joints can be regarded as equivalent spherical joints because their axes intersect at a single point. The spherical joints will be referred to as shoulder (S) and wrist (W) joint, respectively,

in analogy to those of the human arm. In a similar way, the middle joint (Joint #4) will be called the elbow (E) joint. Further on, similar to the human arm, the S-R-S type manipulator comprises two characteristic subchains: the positioning subchain formed by the first four joints with coordinates $q_i, i = 1, 2, 3, 4$, and the orientation subchain formed by the last three (wrist) joints with coordinates $q_j, j = 5, 6, 7$.

A. Kinematic relations for the positioning subchain

When the position and orientation of the end-effector are constrained, then the center position W' of the wrist joint can be determined uniquely from the configuration of the positioning subchain. With the help of the Denavit-Hartenberg notation [15], the position vector can be derived as:

$$ {}^0\boldsymbol{p}_{W'} = \begin{bmatrix} {}^0p_{W'x} \\ {}^0p_{W'y} \\ {}^0p_{W'z} \end{bmatrix} = \begin{bmatrix} \mathrm{C}_1 c - d_5 \mathrm{S}_1 \mathrm{S}_3 \mathrm{S}_4 \\ \mathrm{S}_1 c + d_5 \mathrm{C}_1 \mathrm{S}_3 \mathrm{S}_4 \\ (d_3 + d_5 \mathrm{C}_4)\mathrm{C}_2 - d_5 \mathrm{S}_2 \mathrm{C}_3 \mathrm{S}_4 \end{bmatrix} \quad (1) $$

where $\mathrm{S}_i = \sin q_i$, $\mathrm{C}_i = \cos q_i$, d_3 and d_5 are link lengths and $c = (d_3 + d_5\mathrm{C}_4)\mathrm{S}_2 + d_5\mathrm{C}_2\mathrm{C}_3\mathrm{S}_4$. The respective velocity vector is then:

$$ {}^0\dot{\boldsymbol{p}}_{W'} = \boldsymbol{J}_v \dot{\boldsymbol{q}}_p \quad (2) $$

where $\boldsymbol{q}_p = \begin{bmatrix} q_1 & q_2 & q_3 & q_4 \end{bmatrix}^T$ and $\boldsymbol{J}_v(\boldsymbol{q}_p) \in \mathbb{R}^{3\times 4}$ is the Jacobian of the positioning subchain. The inverse solution can be obtained via the pseudoinverse of the Jacobian, which yields a locally optimized joint velocity solution:

$$ \dot{\boldsymbol{q}}_p = \boldsymbol{J}_v^+ \, {}^0\dot{\boldsymbol{p}}_{W'}. \quad (3) $$

Since the pseudoinverse can be represented as:

$$ \boldsymbol{J}_v^+ = \boldsymbol{J}_v^T \frac{\mathrm{adj}(\boldsymbol{J}_v \boldsymbol{J}_v^T)}{\det(\boldsymbol{J}_v \boldsymbol{J}_v^T)}, \quad (4) $$

it becomes immediately apparent that instabilities will occur at singular configurations where $\det(\boldsymbol{J}_v \boldsymbol{J}_v^T) = 0$. Two types of such singular configurations can be distinguished:

- $\mathrm{S}_2 = 0$ and $\mathrm{C}_3 = 0$,
- $\mathrm{S}_4 = 0$.

The former singularity occurs at internal configurations while the latter one – at the outer workspace boundary of the positioning subchain, when the links are fully extended. In this paper, we focus only on the extended-arm singularity; the internal singularity is easily avoidable with the pseudoinverse solution because of its joint velocity optimization property. The extended-arm singularity (called also *elbow singularity* [19]) cannot be avoided even if self-motion is applied; it is therefore referred to as *unavoidable*. In order to follow any path within the entire workspace, we need to generate joint velocities through (3), hence, the unavoidable elbow singularity must be handled appropriately.

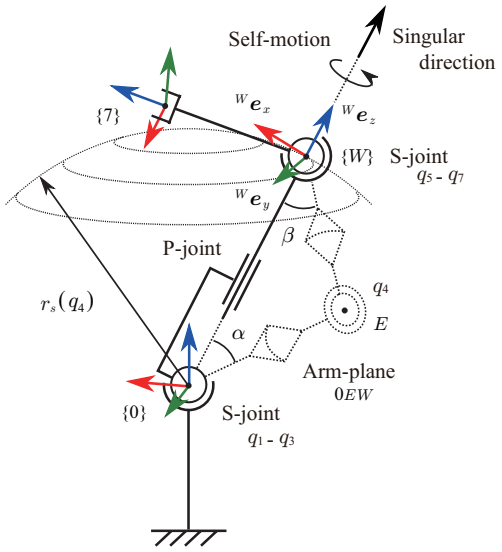

Fig. 2. S-R-S manipulator remodeled with a virtual prismatic joint.

B. Kinematic relations for the orientation subchain

Let ${}^0\boldsymbol{\omega}_{W'}(\dot{\boldsymbol{q}}_p) \in \mathbb{R}^3$ denote the angular velocity of the wrist w.r.t. the base frame. If the end-effector angular velocity ${}^0\boldsymbol{\omega}_7 \in \mathbb{R}^3$ is given, then the wrist joint velocity can be obtained as follows:

$$ \dot{\boldsymbol{q}}_w = \boldsymbol{J}_\omega^{-1\,W'} \boldsymbol{\omega}_7 = \frac{\mathrm{adj}\boldsymbol{J}_\omega}{\det \boldsymbol{J}_\omega}{}^{W'}\boldsymbol{\omega}_7 \quad (5) $$

where $\boldsymbol{q}_w = \begin{bmatrix} q_5 & q_6 & q_7 \end{bmatrix}^T$, the relative angular velocity ${}^{W'}\boldsymbol{\omega}_7 = {}^0\boldsymbol{\omega}_7 - {}^0\boldsymbol{\omega}_{W'}$ and $\boldsymbol{J}_\omega(\boldsymbol{q}_w) \in \mathbb{R}^{3\times 3}$ is the Jacobian matrix for angular motion. From the above equation it is apparent that the orientation subchain is at a singular configuration whenever $\det \boldsymbol{J}_\omega = 0$, that is $\mathrm{S}_6 = 0$. This type of singularity, known as *wrist singularity* [19], is categorized as an unavoidable singularity, as is it was with the elbow singularity [20].

III. A Novel Singularity-Consistent Inverse Kinematics Decomposition

To deal with the unavoidable elbow and wrist singularities, we will introduce an inverse kinematics decomposition scheme based on the Singularity-Consistent method [12]. From past studies it is known that the behavior at a singular point depends on the type of the singular path. A degenerate singular path yields a nonvanishing vector field and hence, a straightforward solution via path reparameterization. A nondegenerate singular path, on the other hand, yields a vanishing vector field at the singularity, thus special measures (switching) had to be introduced [9]. To avoid this drawback, we propose here a novel coordinate transformation.

A. Coordinate transformation for the positioning subchain based on the singular direction

The positioning subchain is remodeled via a kinematically equivalent spherical-prismatic joint (S-P) structure, as shown in Fig. 2. Thereby, the P-joint axis is aligned with the singular

direction. Also, we introduce a new wrist coordinate system $\{W\}$, as follows:

$$ {}^0_W\boldsymbol{R} = \boldsymbol{R}^z(q_1)\boldsymbol{R}^y(q_2)\boldsymbol{R}^z(q_3)\boldsymbol{R}^y(\alpha(q_4)) \tag{6} $$

where $\boldsymbol{R}^z$, $\boldsymbol{R}^y$ denote rotations about z, y axes, respectively, α is derived from

$$ \alpha(q_4) = \mathrm{sgn}(\mathrm{S}_4)\cos^{-1}\left(\frac{d_3 + d_5\mathrm{C}_4}{r_s(q_4)}\right) $$

and $r_s(q_4) = \| {}^0\boldsymbol{p}_W\|$. Note that the z-axis ${}^W\boldsymbol{e}_z$ of coordinate system $\{W\}$ points along the singular direction. With this model, the singular direction becomes available in base coordinates:

$$ {}^0\boldsymbol{e}_z = {}^0_W\boldsymbol{R}\,{}^W\boldsymbol{e}_z. \tag{7} $$

Note also that $r_s(q_4)$ can be used as an elbow singularity index.

Further on, as shown in Fig. 2, the self motion of the positioning subchain can be defined as a rotation around the singular direction. The null-space vector $\boldsymbol{n}_{sm}$ that produces the self motion is derived from the kernel of $\boldsymbol{J}_v$:

$$ \boldsymbol{n}_{sm} = \begin{bmatrix} -d_5\mathrm{C}_3\mathrm{S}_4 \\ d_5\mathrm{S}_2\mathrm{S}_3\mathrm{S}_4 \\ c \\ 0 \end{bmatrix} \in \mathrm{Ker}\boldsymbol{J}_v. \tag{8} $$

With these preparations, we rewrite the velocity relation for the positioning chain as follows:

$$ {}^W\dot{\boldsymbol{p}}_W = {}^0_W\boldsymbol{R}^T\boldsymbol{J}_v\dot{\boldsymbol{q}}, \tag{9} $$

where ${}^W\dot{\boldsymbol{p}} = [{}^W\dot{p}_{Wx}\ {}^W\dot{p}_{Wy}\ {}^W\dot{p}_{Wz}]^T$ stands for the velocity of the wrist center point w.r.t $\{W\}$. Denote ${}^0_W\boldsymbol{R}^T\boldsymbol{J}_v$ as:

$$ {}^W\boldsymbol{J}_v = \begin{bmatrix} r_s\mathrm{S}_2\mathrm{S}_3 & r_s\mathrm{C}_3 & 0 & d_5\mathrm{C}_\beta \\ (d_3 + d_5\mathrm{C}_4)\mathrm{S}_2\mathrm{C}_3 + d_5\mathrm{C}_2\mathrm{S}_4 & (d_3 + d_5\mathrm{C}_4)\mathrm{S}_3 & d_5\mathrm{S}_4 & 0 \\ 0 & 0 & 0 & -d_5\mathrm{S}_\beta \end{bmatrix} \tag{10} $$

where $\mathrm{S}_\beta = \sin\beta$, $\mathrm{C}_\beta = \cos\beta$ and β is derived as:

$$ \beta(q_4) = \mathrm{sgn}(\mathrm{S}_4)\cos^{-1}\left(\frac{d_3\mathrm{C}_4 + d_5}{r_s(q_4)}\right). \tag{11} $$

With this transformation, velocity component ${}^W\dot{p}_{Wz}$ produces a motion along the singular direction. This means that the other two components, ${}^W\dot{p}_{Wx}$ and ${}^W\dot{p}_{Wy}$, will never contribute a motion toward the elbow singularity; they produce a motion only along a non-singular direction. This provides the basis of our decomposition scheme.

First, we define the following joint velocity vector component for the positioning subchain:

$$ \dot{\boldsymbol{q}}_{xy} = [{}^W\bar{\boldsymbol{J}}_v]^+ \begin{bmatrix} {}^W\dot{p}_{Wx} \\ {}^W\dot{p}_{Wy} \end{bmatrix} \in \mathbb{R}^4 \tag{12} $$

where ${}^W\bar{\boldsymbol{J}}_v \in \mathbb{R}^{2\times 4}$ is obtained from ${}^W\boldsymbol{J}_v$ by removing the third line. With this joint velocity, the wrist center is restricted to move only within the spherical surface defined by the current r_s, as shown in Fig. 2. Hence, the joint velocity component producing a motion along the singular direction can be derived from the kernel of ${}^W\bar{\boldsymbol{J}}_v$:

$$ \dot{\boldsymbol{q}}_z = b_z\,{}^W\dot{p}_{Wz}\,{}^W\boldsymbol{n}_z, \quad {}^W\boldsymbol{n}_z \in \mathrm{Ker}{}^W\bar{\boldsymbol{J}}_v, \tag{13} $$

where b_z denotes an arbitrary scalar to be determined later. Since the kernel is two-dimensional, there are an infinite number of choices for vector $\boldsymbol{n}_z$. To obtain the joint velocity based on the original pseudoinverse map in (3), we choose ${}^W\boldsymbol{n}_z$ to be orthogonal to $\boldsymbol{n}_{sm}$, hence:

$$ {}^W\boldsymbol{n}_z = \frac{1}{d_3\mathrm{S}_4\det({}^W\boldsymbol{J}_v\,{}^W\boldsymbol{J}_v{}^T)} \begin{bmatrix} {}^Wn_{z1} \\ {}^Wn_{z2} \\ {}^Wn_{z3} \\ {}^Wn_{z4} \end{bmatrix}, \tag{14} $$

where the components are:

$$ \begin{aligned} {}^Wn_{z1} &= {r_s}^2\mathrm{C}_\beta\mathrm{S}_3\left(\mathrm{S}_2 + \mathrm{S}_\alpha\mathrm{C}_\alpha\mathrm{C}_2\mathrm{C}_3\right), \\ {}^Wn_{z2} &= {r_s}^2\mathrm{C}_\beta\left(2\mathrm{S}_\alpha^2\mathrm{C}_2^2\mathrm{C}_3 + \mathrm{S}_2^2\mathrm{C}_3 \right. \\ &\qquad \left. +\mathrm{S}_\alpha\mathrm{C}_\alpha\mathrm{S}_2\mathrm{C}_2\left(1 + \mathrm{C}_3^2\right)\right), \\ {}^Wn_{z3} &= {r_s}^2\mathrm{C}_\beta\mathrm{C}_2\mathrm{S}_3\mathrm{S}_\alpha\left(\mathrm{C}_2\mathrm{C}_3\mathrm{C}_\alpha - \mathrm{S}_2\mathrm{S}_\alpha\right), \\ {}^Wn_{z4} &= -d_3\mathrm{S}_4\det({}^W\boldsymbol{J}_v\,{}^W\boldsymbol{J}_v{}^T)/d_5. \end{aligned} $$

$\mathrm{S}_\alpha = \sin\alpha$, $\mathrm{C}_\alpha = \cos\alpha$, and

$$ \begin{aligned} \det({}^W\boldsymbol{J}_v\,{}^W\boldsymbol{J}_v{}^T) &= {\boldsymbol{n}_{sm}}^T\boldsymbol{n}_{sm} \\ &= c^2 + {d_5}^2{\mathrm{S}_4}^2({\mathrm{C}_3}^2 + {\mathrm{S}_2}^2{\mathrm{S}_3}^2). \end{aligned} \tag{15} $$

Note that the vector part of equation (14) never diverges throughout the inverse calculation. On the other hand, from the scalar part it is apparent that joint velocity component $\dot{\boldsymbol{q}}_z$ cannot be obtained when $\det({}^W\boldsymbol{J}_v\,{}^W\boldsymbol{J}_v{}^T) = 0$ or $\mathrm{S}_4 = 0$. Note that the former condition implies $\mathrm{S}_2 = 0$ and $\mathrm{C}_3 = 0$. This is an avoidable type of singularity; it never occurs because we use the pseudoinverse property, as discussed in the previous section.

B. Application of the Singularity-Consistent method

The Singularity-Consistent method [12] provides an inverse kinematics solution wherein the singular point can be approached without any directional error with a stable joint velocity obtained by restricting appropriately the magnitude of the end-effector velocity. In terms of the decomposition scheme developed so far, the restriction is applied to the

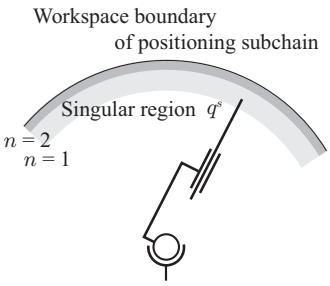

Fig. 3. Singular region.

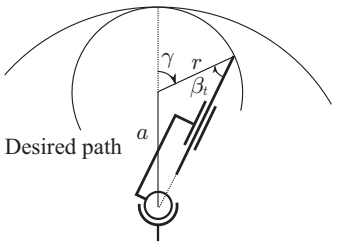

Fig. 4. Circular path parameters.

motion generated via vector field ${}^W\boldsymbol{n}_z$. This can be done by determining the arbitrary scalar b_z in (13) to be dependent upon the distance from the current point to the workspace boundary. We should note though that from a practical point, velocity limitation is not preferable. Therefore, we will apply the method only when the wrist center reaches the vicinity of the elbow singularity. The vicinity is defined in terms of elbow coordinate q_4 as:

$$q^s \equiv \{\varepsilon \geq |S_4|\} \tag{16}$$

where $\varepsilon > 0$ is a threshold defined below. Within the vicinity, b_z is determined to include S_4 and hence, to cancel the unstable denominator:

$$b_z = \begin{cases} \sin(2^n q_4), & \text{if } \ q_4 \in q^s, \\ \mathrm{sgn}(\mathrm{S}_4), & \text{otherwise.} \end{cases} \tag{17}$$

Factor 2^n has been included to ensure a smooth transition when entering/leaving the singularity region. Integer n determines the range of the singularity region (shown in Fig. 3). ε is defined as:

$$\varepsilon \equiv \sin(\pi/4n). \tag{18}$$

Although b_z becomes zero when the wrist center reaches the workspace boundary, a nondegenerate vector field (a nonzero vector ${}^W\boldsymbol{n}_z$) exists in joint space. That is, ${}^W\boldsymbol{n}_z$ instantaneously becomes a nullspace vector, and therefore, it becomes possible to obtain the inverse solution at the elbow singularity.

IV. The Complete Solution

As a result of the above transformations we obtained three components of the joint velocity for the positioning subchain. That is, instead of the conventional pseudoinverse solution (3), we propose the following decomposition:

$$\begin{aligned} \dot{\boldsymbol{q}}_p &= \dot{\boldsymbol{q}}_{xy} + \dot{\boldsymbol{q}}_z + b_{sm}\boldsymbol{n}_{sm} \\ &= [{}^W\bar{\boldsymbol{J}}_v]^+ \begin{bmatrix} {}^W\dot{p}_{Wx} \\ {}^W\dot{p}_{Wy} \end{bmatrix} + b_z\, {}^W\boldsymbol{n}_z\, {}^W\dot{p}_{Wz} + b_{sm}\boldsymbol{n}_{sm}, \end{aligned} \tag{19}$$

where b_{sm} is an arbitrary scalar to be used as control input for generating self motion. Note that the motion along the singular direction depends on the sign of S_4: after reaching the singularity (where $\mathrm{S}_4 = 0$), the sign changes and hence, the motion is reversed. This means the wrist center will "reflect" from the workspace boundary along the desired path. The reference value ${}^W\dot{p}_z^{ref}$ should include this information, hence:

$${}^W\dot{p}_{Wz}^{ref} = \begin{cases} {}^W\dot{p}_{Wz}^{des}, & \text{if } \ S_4 = 0, \\ \mathrm{sgn}(\mathrm{S}_4)\, {}^W\dot{p}_{Wz}^{des}, & \text{otherwise.} \end{cases} \tag{20}$$

${}^W\dot{p}_{Wz}^{des}$ is the desired value of the wrist speed along the singular direction. Although the SC approach restricts this speed and introduces therefore an algorithmic error, this happens only within a small region. A proper *path following controller* can be designed because the motion direction can be followed precisely, without any directional error. Furthermore, note that with the above decomposition, no errors will be introduced for the nonsingular directions. For these directions, the controller will have the property of a *path tracking controller*. Moreover, the appearance of an "inner obstacle" as reported in [18], can be avoided because of the pseudoinverse property. These are two major improvements of our previous result.

Let us now focus on the orientation subchain and discuss how to obtain the wrist joint velocity $\dot{\boldsymbol{q}}_w$ while dealing with the unavoidable wrist singularity $S_6 = 0$. As discussed above, one of the advantages of our approach is that we can handle the self motion independently in terms of position. This cannot be achieved with the Singularity-Consistent method when using conventional modeling [18]. To alleviate the wrist singularity problem, we introduce self motion w.r.t. orientation, thus representing the orientation subchain by a four DOF subsystem. The relation is given as follows[1]:

$${}^W\boldsymbol{\omega}_7 = \boldsymbol{R}^y(\beta)\boldsymbol{J}_\omega\dot{\boldsymbol{q}}_w + \boldsymbol{\omega}_{sm} = \bar{\boldsymbol{J}}_\omega\dot{\bar{\boldsymbol{q}}}_w, \tag{21}$$

where $\boldsymbol{\omega}_{sm}$ denotes the self-motion angular velocity, and $\bar{\boldsymbol{J}}_\omega$ and $\dot{\bar{\boldsymbol{q}}}_w$ are defined as

$$\bar{\boldsymbol{J}}_\omega = \begin{bmatrix} \mathrm{S}_\beta & -\mathrm{C}_\beta\mathrm{S}_5 & \mathrm{S}_\beta\mathrm{C}_6 + \mathrm{C}_\beta\mathrm{C}_5\mathrm{S}_6 & 0 \\ 0 & \mathrm{C}_5 & \mathrm{S}_5\mathrm{S}_6 & 0 \\ \mathrm{C}_\beta & \mathrm{S}_\beta\mathrm{S}_5 & \mathrm{C}_\beta\mathrm{C}_6 - \mathrm{S}_\beta\mathrm{C}_5\mathrm{S}_6 & r_s\mathrm{S}_2 \end{bmatrix},$$
$$\dot{\bar{\boldsymbol{q}}}_w = \begin{bmatrix} \dot{\boldsymbol{q}}_w & \dot{q}_{sm} \end{bmatrix}^T.$$

$\dot{q}_{sm}$ denotes angular speed around the singular direction, that is, the role of this parameter is the same as that of b_{sm}. The wrist joint velocity can be obtained from (21) via the pseudoinverse mapping:

$$\dot{\bar{\boldsymbol{q}}}_w = [\bar{\boldsymbol{J}}_\omega]^+ {}^W\boldsymbol{\omega}_7. \tag{22}$$

Note that Jacobian $\bar{\boldsymbol{J}}_\omega$ looses rank when $\mathrm{S}_2 = 0$ and $\mathrm{S}_6 = 0$. In this way, the unavoidable wrist singular configuration was transformed to an internal (avoidable) singularity, and therefore, will be automatically avoided due to the property of the pseudoinverse map. The only exception is the double wrist-elbow singularity: $\mathrm{S}_2 = 0$, $\mathrm{S}_4 = 0$ and $\mathrm{S}_6 = 0$. This condition can occur only at an isolated point at the workspace boundary - fully extended-arm along the vertical.

V. Numerical experiments

To realize end-effector motion without directional error within the entire workspace, the b_z scale factor of the singular direction should be also applied to the non-singular direction component. Hence, the following inverse kinematics decomposition will be used for the positioning subchain:

$$\dot{\boldsymbol{q}}_p = b_z \left([{}^W\bar{\boldsymbol{J}}_v]^+ \begin{bmatrix} {}^W\dot{p}_{Wx} \\ {}^W\dot{p}_{Wy} \end{bmatrix} + {}^W\boldsymbol{n}_z\, {}^W\dot{p}_{Wz} \right) + \dot{q}_{sm}\boldsymbol{n}_{sm}. \tag{23}$$

Note that self motion is utilized to avoid wrist singularities with the help of parameter $\dot{q}_{sm}$. This parameter is obtained by solving (22) first. With this scheme, the angular motion will also be constrained within the singularity region. At the singularity, both translational and rotational motion will

[1]Note that the description (21) is based on the wrist coordinate defined in (6), therefore, it is different from that discussed in Section II-B.

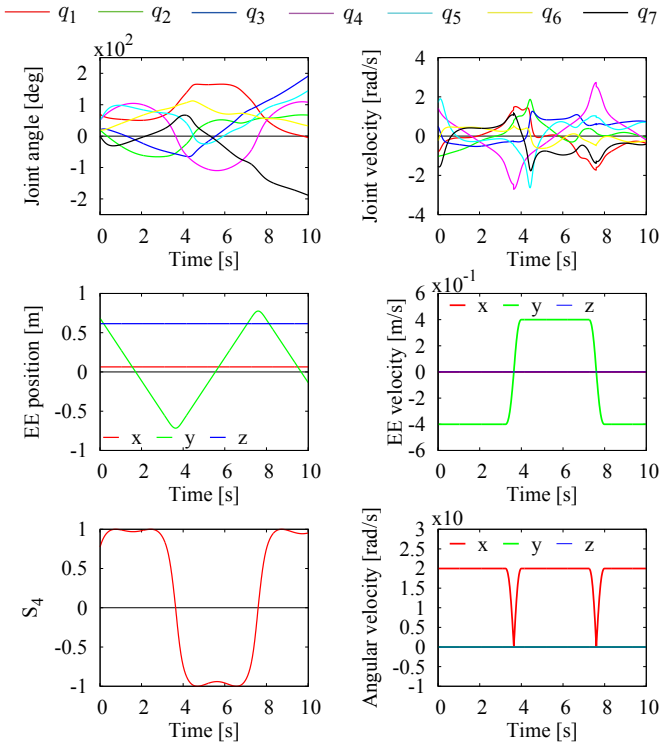

Fig. 5. The desired path of the end-effector is parallel to the y-axis of the base frame. Simulation results illustrate that the motion can be generated without unstable conditions in the singularity neighborhood, i.e. joint velocity can be obtained when approaching and moving away from the elbow singularity.

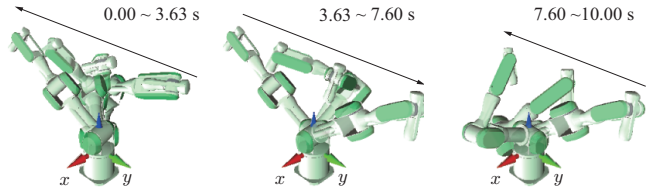

Fig. 6. A singular degenerate path case study: the end-effector translates along the y-axis and rotates around the x-axis, moving thereby through the elbow singularity at $t = 3.63$ s and $t = 7.6$ s.

pause instantaneously, and then "reflect" back from the workspace boundary along the desired path to their desired values. The singularity region definition parameter is $n = 2$ ($\varepsilon = 0.38268$). Link lengths are $d_3 = 0.45$ m, $d_5 = 0.5$ m and $d_7 = 0.08$ m. The simulation time is set to 10 s.

A. Singular degenerate path (straight-line segment)

First, we verify the precise path following capability for a singular degenerate path passing through the elbow singularity. The initial joint angles are given as $\boldsymbol{q}(0) = \begin{bmatrix}70 & 20 & 20 & 50 & 50 & 20 & 0\end{bmatrix}^T$ deg. The desired path includes a translational component parallel to the y-axis and a rotational component with desired angular velocity direction parallel to the x-axis, all defined w.r.t. the base $\{0\}$ frame. The magnitudes of the end-effector velocity and angular velocity to be maintained within the non-singular portion of workspace are $\| {}^0\dot{\boldsymbol{p}}_7\| = 0.4$ m/s and $\| {}^0\boldsymbol{\omega}_7\| = 0.2$ rad/s, respectively.

Results from the simulation are shown in Figs. 5 and 6. From the results it becomes apparent that the wrist center passes two times through the elbow singularity without any destabilization. Also, the end-effector *directions* for path tracking and angular motion are maintained without any error. The magnitudes of the end-effector velocity and angular velocity are modified only within the singularity region, to obtain the singularity-consistent solution.

B. Singular nondegenerate path (circular arc)

The Singularity-Consistent method reported in our past study on S-R-S manipulator could not handle such paths [18]. Because of this, a motion through a bifurcation-type singularity [11] has not been realized. This becomes possible with the proposed method, as will be verified via the following numerical simulation.

To generate a motion through a singularity along the nonsingular direction, the desired wrist center path should be tangent to the workspace boundary. We define therefore a circular path, as shown in Fig. 4. The following path parameters are introduced: $a, r > 0$ and $\beta_t, \gamma \in (-\pi, \pi]$, their meaning being apparent from the figure. The elbow singularity index S_4 can be then rewritten as:

$$\mathrm{S}_4 = \pm 2 \cos\frac{q_4}{2} k \sin\frac{\gamma}{2}, \tag{24}$$

where $k = \sqrt{ar/(d_3 d_5)}$. The sign of (24) depends on the manipulator configuration. At the elbow singularity, $\sin(\gamma/2)$ is equal to zero and will be used as a singularity index instead of S_4. On the other hand, ${}^W\dot{p}_W$ is defined by the path parameters as follows:

$${}^W\dot{p}_{Wz} = \|{}^W\dot{\boldsymbol{p}}_W\| \sin\beta_t = \|{}^W\dot{\boldsymbol{p}}_W\| \left(\frac{a}{r_s}\right) 2 \sin\frac{\gamma}{2}\cos\frac{\gamma}{2}, \tag{25}$$

${}^W\dot{p}_{Wz}$ includes $\sin(\gamma/2)$, and hence, we apply it to cancel the singularity factor.

In this simulation, for clarity we will consider only the positioning subchain. The initial configuration is $\boldsymbol{q}_p(0) = \begin{bmatrix}143.973 & -137.310 & 0 & 88.727\end{bmatrix}^T$ deg. The path parameters are given as: $r = 0.4$ m; γ starts from -90 deg toward 90 deg on the x-y plane; the end-effector moves with constant speed along the path and reaches the goal at 10 s. Also, the sign of (24) is negative.

The simulation results are shown in Fig. 7 and respective snapshots — in Fig. 8. From the results it is apparent that the end-effector follows the desired path without errors and passes through the elbow singularity along the tangential direction to the outer workspace boundary without destabilization.

VI. Conclusions

We proposed an inverse kinematics decomposition scheme for S-R-S type manipulators at the velocity level. Results from a previous study based on the Singularity-Consistent

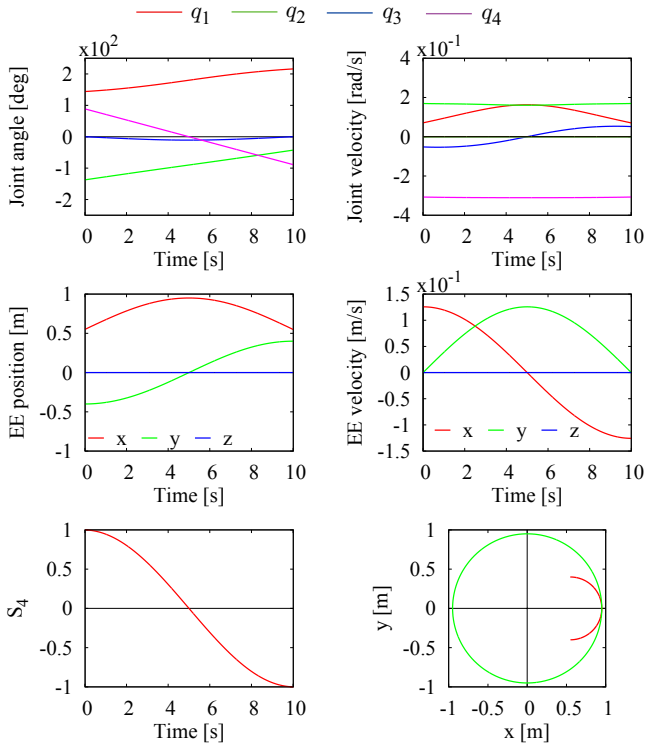

Fig. 7. Simulation results illustrate that the motion can be generated in a stable way even when the end-effector follows a path tangent to the outer workspace boundary.

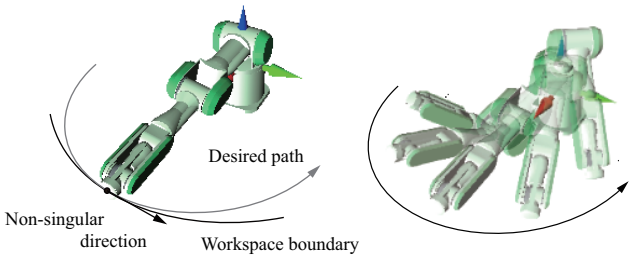

Fig. 8. A singular nondegenerate path case study: the end-effector follows the desired circular path and moves in the non-singular direction at the elbow singularity.

method have been extended as follows. First, it became possible to follow nondegenerate singular paths in addition to degenerate singular paths. Second, the problem of the "inner obstacle" was alleviated with the help of the local minimization property of the pseudoinverse component. The problem of wrist singularity was also addressed and solved via the self motion component. As a result, the manipulator becomes capable of following the position and orientation components of almost any path within the entire workspace, provided a proper path parametrization (for the nonsingular direction) can be found. Only a limited subset of singular paths cannot be handled: those that pass through the double elbow-wrist singularity, which is an isolated point (the "north pole") at the workspace boundary. Motion planners do not have to be restricted anymore to avoid kinematic singularities, and a larger effective workspace can be achieved. Such capabilities are essential for such tasks as teleoperation and inspection with an eye-in-hand system. The proposed scheme can also be applied to other types of manipulators comprising a triangular arm-plane, e.g. nonredundant planar 2R manipulators and spatial 3R ones.

REFERENCES

[1] K. Oonishi, "The open manipulator system of the MHI PA-10 robot," in *Proc. of the 30th Int. Symp. of Robotics*, 1999.

[2] R. Bischoff, J. Kurth, G. Schreiber, R. Koeppe, A. Albu-Schäffer, A. Beyer, O. Eiberger, S. Haddadin, A. Stemmer, G. Grunwald, and G. Hirzinger, "The KUKA-DLR Lightweight Robot arm a new reference platform for robotics research and manufacturing," in *ISR/ROBOTIK*, 2010, pp. 741–748.

[3] K. Kaneko, K. Harada, F. Kanehiro, G. Miyamori, and K. Akachi, "Humanoid robot HRP-3," in *IEEE/RSJ Int. Conf. on Intelligent Robots and Syst.*, 2008, pp. 2471–2478.

[4] C. Borst, T. Wimbock, F. Schmidt, M. Fuchs, B. Brunner, F. Zacharias, P. R. Giordano, R. Konietschke, W. Sepp, S. Fuchs, C. Rink, A. Albu-Schaffer, and G. Hirzinger, "Rollin' Justin - Mobile platform with variable base," in *IEEE Int. Conf. on Robotics and Automation*, May 2009, pp. 1597–1598.

[5] Y. Nakamura and H. Hanafusa, "Inverse kinematic solutions with singularity robustness for robot manipulator control," *J. of Dynamic Syst., Measurement, and Control*, vol. 108, pp. 163–171, 1984.

[6] C. Wampler, "Manipulator inverse kinematic solutions based on vector formulations and damped least-squares methods," *IEEE Trans. on Syst., Man., and Cybern.*, vol. 16, no. 1, pp. 93–101, 1986.

[7] J. Xiang, C. Zhong, and W. Wei, "General-weighted least-norm control for redundant manipulators," *IEEE Trans. on Robotics*, vol. 26, no. 4, pp. 660–669, 2010.

[8] T. Sugihara, "Solvability-unconcerned inverse kinematics by the Levenberg-Marquardt method," *IEEE Trans. on Robotics*, vol. 27, no. 5, pp. 984–991, 2011.

[9] D. Nenchev, Y. Tsumaki, and M. Uchiyama, "Singularity-Consistent parameterization of robot motion and control," *The Int. J. of Robotics Research*, vol. 19, no. 2, pp. 159–182, 2000.

[10] D. Oetomo and M. Ang, "Singularity robust algorithm in serial manipulators," *Robotics and Comput.-Integrated Manufacturing*, vol. 25, no. 1, pp. 122–134, 2009.

[11] J. Kieffer, "Differential analysis of bifurcations and isolated singularities for robots and mechanisms," *IEEE Trans. on Robotics and Automation*, vol. 10, no. 1, pp. 1–10, 1994.

[12] D. Nenchev, "Tracking manipulator trajectories with ordinary singularities: a null space-based approach," *The Int. J. of Robotics Research*, vol. 14, no. 4, pp. 399–404, 1995.

[13] S. B. Nokleby and R. P. Podhorodeski, "Reciprocity-based resolution of velocity degeneracies (singularities) for redundant manipulators," *Mechanism and Machine Theory*, vol. 36, no. 3, pp. 397–409, 2001.

[14] ——, "Identifying multi-DOF-loss velocity degeneracies in kinematically-redundant manipulators," *Mechanism and Machine Theory*, vol. 39, no. 2, pp. 201–213, 2004.

[15] M. Shimizu, H. Kakuya, W.-K. Yoon, K. Kitagaki, and K. Kosuge, "Analytical inverse kinematic computation for 7-DOF redundant manipulators with joint limits and its application to redundancy resolution," *IEEE Trans. on Robotics*, vol. 24, no. 5, pp. 1131–1142, 2008.

[16] C. Yu, M. Jin, and H. Liu, "An analytical solution for inverse kinematic of 7-DOF redundant manipulators with offset-wrist," in *IEEE Int. Conf. on Mechatron. and Automation*, 2012, pp. 92–97.

[17] J. Kim, G. Marani, W. K. Chung, and J. Yuh, "Task reconstruction method for real-time singularity avoidance for robotic manipulators," *Advanced Robotics*, vol. 20, no. 4, pp. 453–481, 2006.

[18] D. Nenchev, Y. Tsumaki, and M. Takahashi, "Singularity-consistent kinematic redundancy resolution for the S-R-S manipulator," *IEEE/RSJ Int. Conf. on Intelligent Robots and Syst.*, vol. 4, pp. 3607–3612, 2004.

[19] K. Kreutz-Delgado, M. Long, and H. Seraji, "Kinematic analysis of 7-DOF manipulators," *The Int. J. of Robotics Research*, vol. 11, no. 5, pp. 469–481, 1992.

[20] N. Bedrossian, "Classification of singular configurations for redundant manipulators," in *Proc. IEEE Int. Conf. on Robotics and Automation*. IEEE Comput. Soc. Press, 1990, pp. 818–823.